

Dynamics of anoxygenic photosynthesis in an experimental green sulphur bacteria biofilm

Olivier Pringault,^{1*} Eric Epping,¹ Remy Guyoneaud,² Arzhang Khalili¹ and Michael Kühl¹

¹Max Planck Institute for Marine Microbiology, Microsensor Research Group, Celsiusstraße 1, D-28359 Bremen, Germany.

²Institute of Aquatic Ecology, University of Girona, Campus de Montilivi, E-17071 Girona, Spain.

Summary

The dynamics of sulphide oxidation in an experimental biofilm of the green sulphur bacterium, *Prosthecochloris aestuarii*, were studied using a newly developed light–dark cycling procedure. The biofilm was grown for 6 weeks in a benthic gradient chamber, in which gradients of light, sulphide and oxygen were imposed experimentally. The H₂S concentrations and pH were measured with microsensors as a function of depth in the biofilm and of time after a change in illumination status. The sulphide oxidation rates were calculated as a function of time and depth in the biofilm using a numerical procedure to solve the non-stationary general diffusion equation. A close agreement was found between the areal rates of anoxygenic photosynthesis during the cycling procedure and the steady state before the cycling experiment. For the different layers of the biofilm, the maximum activity was observed after 10–12 min of light exposure. After this maximum, sulphide oxidation decreased concomitantly with sulphide concentration, indicating sulphide limitation of anoxygenic photosynthesis. This lag time limits the application of the standard dark–light shift method with a brief light exposure of a few seconds and, therefore, the numerical procedure described in this study enables the depth distribution of anoxygenic photosynthesis rates in microbial mats to be determined more accurately.

Introduction

Anoxygenic photosynthesis is one of the major biological processes of the sulphur cycle. In benthic systems, the

sulphide production resulting from the activity of sulphate-reducing bacteria can be very intense, especially in microbial mats, in which sulphide production rates of 100 mmol of H₂S m⁻² day⁻¹ have been measured (Skyring, 1987). The biological reoxidation of sulphide to sulphate is performed by two main groups of bacteria, the sulphur-oxidizing bacteria and the phototrophic sulphur bacteria (Van Gemerden, 1993). The chemical oxidation of sulphide is a rather slow process that can be enhanced in sediments by the presence of trace metals, e.g. iron and manganese (King, 1990; Millero, 1991; Thamdrup *et al.*, 1993). If sufficient light is present and oxygen levels are low, anoxygenic photosynthesis is the main microbiological pathway of sulphide oxidation (Jørgensen and Des Marais, 1986; Visscher *et al.*, 1992).

Phototrophic sulphur bacteria are divided phenotypically into two groups, purple sulphur bacteria and green sulphur bacteria. The green sulphur bacteria are obligate anaerobes, and their growth is entirely inhibited by the presence of trace amounts of molecular oxygen (Van Gemerden and Mas, 1995). It has been suggested that oxygen inhibition reduces the ability of green sulphur bacteria to thrive in microbial mats because of the oxygen production by the phototrophic microorganisms (Van Gemerden, 1993). However, some microbial mats in salt marshes have been described in which the lowermost layers were composed mainly of the green sulphur bacterium *Prosthecochloris* (Nicholson *et al.*, 1987; Pierson *et al.*, 1987; 1990; Stolz, 1990).

Sulphide oxidation rates can be assessed by comparing steady-state sources and sinks for sulphide for the depth interval of interest. In illuminated microbial communities, sulphate reduction and sulphide fluxes into the layer can be qualified as sources, whereas sulphide oxidation and fluxes out of the layer are to be considered as sinks. This steady-state approach has been adopted in a number of studies (Kühl and Jørgensen, 1992a; Pringault *et al.*, 1996; 1998; Fenchel, 1998). The dark–light shift method, originally described by Revsbech and Jørgensen (1983) to measure gross photosynthesis, has been applied to estimate the anoxygenic photosynthesis in a hypersaline microbial mat (Caumette *et al.*, 1994). The potentiometric sensor used in this study, however, does not allow a measurement of the sulphide oxidation with a high spatial resolution on account of its long response time. Therefore, in spite of the importance of anoxygenic photosynthesis

Received 3 February, 1999; revised 8 March, 1999; accepted 11 March, 1999. *For correspondence. E-mail opringau@mpi-bremen.de; Tel. (+49) 421 2028 630; Fax (+49) 421 2028 580.

for the sulphur cycle, no standard method is currently available to estimate this process in undisturbed microbial communities.

The aim of this study was to estimate the rate of anoxygenic photosynthesis in an experimental biofilm of *P. aestuarii*. The biofilm of *P. aestuarii* was grown in the benthic gradient chamber (BGC), a device designed to cultivate phototrophic microorganisms in experimental benthic gradients (Pringault *et al.*, 1996; 1998). The rate of anoxygenic photosynthesis was estimated from the dynamics in sulphide concentration upon the onset of illumination. The experimental procedure and the numerical procedures to solve the non-steady-state diffusion reaction equations have been described by E. Epping *et al.* (unpublished).

Results

*H*₂S diffusion measurements

For this study, knowledge of the apparent diffusion coefficient for free sulphide was essential. The sulphide microsensor measures H₂S only, which represents 23% of the total sulphide at the experimental pH of 7.2 (Stumm and Morgan, 1981; Millero *et al.*, 1988). The total sulphide concentration S_t ($S_t = [H_2S] + [HS^-] + [S^{2-}]$) was calculated from the pH value and the reading of the H₂S microsensor (for more details, see Pringault *et al.*, 1998). A steady-state sulphide profile as measured in the diffusion chamber is shown Fig. 1B. The ratio of concentration gradient in the sediment and agar phase was 4.39. After correction for the sediment porosity of 0.5 and by assuming a free solution diffusion coefficient in agar, the D_s value deduced from this ratio was $7.52 \times 10^{-6} \text{ cm}^2 \text{ s}^{-1}$. Three other profiles yielded values for D_s of $8.02 \times 10^{-6} \text{ cm}^2 \text{ s}^{-1}$, $7.40 \times 10^{-6} \text{ cm}^2 \text{ s}^{-1}$ and $7.29 \times 10^{-6} \text{ cm}^2 \text{ s}^{-1}$. This gives an average value of $D_s = 7.46 \times 10^{-6} \text{ cm}^2 \text{ s}^{-1}$ ($\pm 0.32 \times 10^{-6}$; $n = 4$).

Biofilm location and chemical profiles

The biofilm location and the profiles of oxygen, sulphide and pH in the dark and in the light are shown Fig. 2. The location of the biofilm, as deduced from the attenuation radiance for 750 nm, showed a bimodal distribution. From the sediment–water interface down to 2 mm depth, the radiance attenuation was approximately equal to the abiotic value, indicating the absence of the specific photopigment. The biofilm was located between 2 and 3.6 mm with a maximum in Bchl *c* concentration at 3 mm depth. In the light, the sulphide front was observed at a depth of 3.2 mm (i.e. the uppermost sediment horizon in which sulphide was detected). The maximum oxygen penetration was 1.9 mm. As a result, a zone without sulphide and oxygen was located between 1.9 and 3.2 mm (Fig. 2A). The

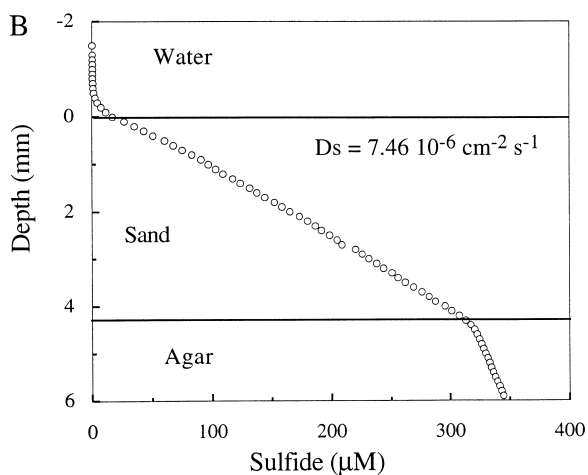
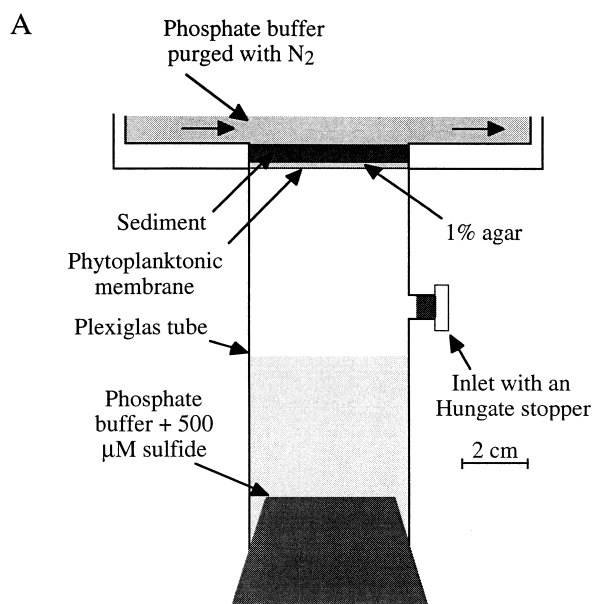


Fig. 1. Estimation of the whole-sediment diffusion coefficient D_s for H₂S.

A. Schematic representation of the diffusion chamber.

B. Concentration gradients of sulphide in the sterile sand.

pH was almost constant with depth. The sulphide flux amounted to $0.079 \text{ nmol cm}^{-2} \text{ s}^{-1}$. In the dark, anoxygenic photosynthesis stopped and, as a consequence, sulphide diffused up to the surface (Fig. 2B). After a few hours of dark exposure, sulphide and oxygen co-existed within a layer of 1.4 mm, thus confirming the absence of chemosynthetic activity of the bacteria to oxidize sulphide with oxygen as electron acceptor, as described previously (Pringault *et al.*, 1998).

Light–dark cycles

The efficiency of the phosphate buffer was checked during the light–dark cycles. The pH and sulphide variations at a

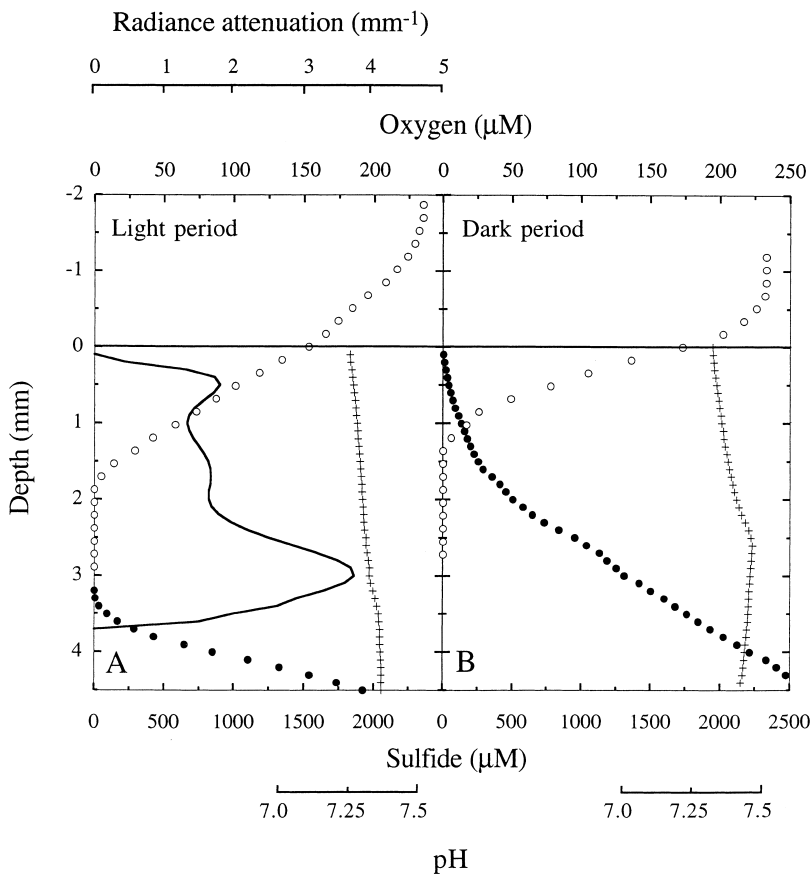


Fig. 2. Oxygen (\circ), sulphide (\bullet) and pH ($+$) steady-state microprofiles measured in the light and in the dark period in a biofilm of *Prosthecochloris aestuarii*. The radiance attenuation (solid line) is also depicted to visualize the bacteria distribution.

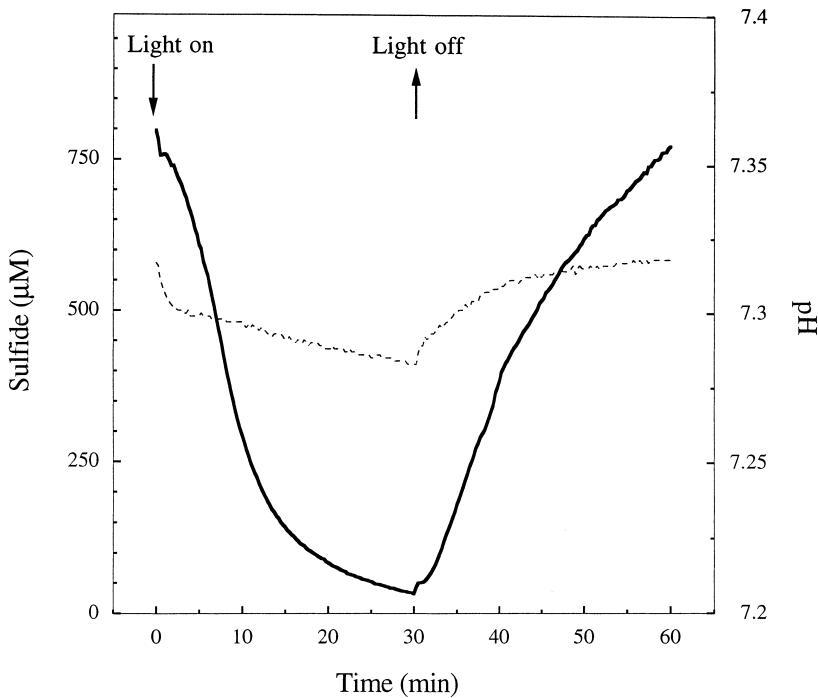


Fig. 3. Sulphide (solid line) and pH (dotted line) variations at 2.8 mm below the sand surface during a light-dark shift in a biofilm of *Prosthecochloris aestuarii*.

depth of 2.8 mm (i.e. within the biofilm) during a light–dark cycle of 30 min are shown in Fig. 3. In the light period, sulphide decreased, whereas pH did not change significantly. When the light was turned off, the photosynthetic sulphide oxidation stopped and, within 30 min, the sulphide concentration increased to approximately the concentration observed at the start of the light period. During darkness, the pH was constant with time (Fig. 3). Figure 4 shows the sulphide concentration as a function of time for a number of depths within the biofilm. Upon light exposure, the sulphide concentration immediately decreased for the layers between 2.6 and 3.2 mm. At depths from 2.0 to 2.6 mm, a time lag was observed before sulphide decreased. This lag was more pronounced for the top of the biofilm (i.e. 2.0 mm). After a light exposure of 30 min, sulphide was available for the deepest layers of the biofilm only, and

steady-state conditions were almost attained. Upon darkening, the sulphide concentration increased to the values observed at the start of the light period.

The light–dark cycle data can be represented as transient sulphide profiles, which are obtained by plotting the sulphide concentration versus depth for a defined time after a change to light or darkness. A total of 240 profiles was reconstructed for the entire experiment. A selection of transient profiles is depicted in Fig. 4B and C. The transition from darkness to light clearly showed a high sulphide consumption between 2.8 and 3.4 mm, whereas in the uppermost layers, the sulphide oxidation was much lower (Fig. 4B). In darkness, the sulphide increase appeared to be uniform with depth, with no indication of sulphide production layers. The absence of sulphide production zones was confirmed by numerical analysis of

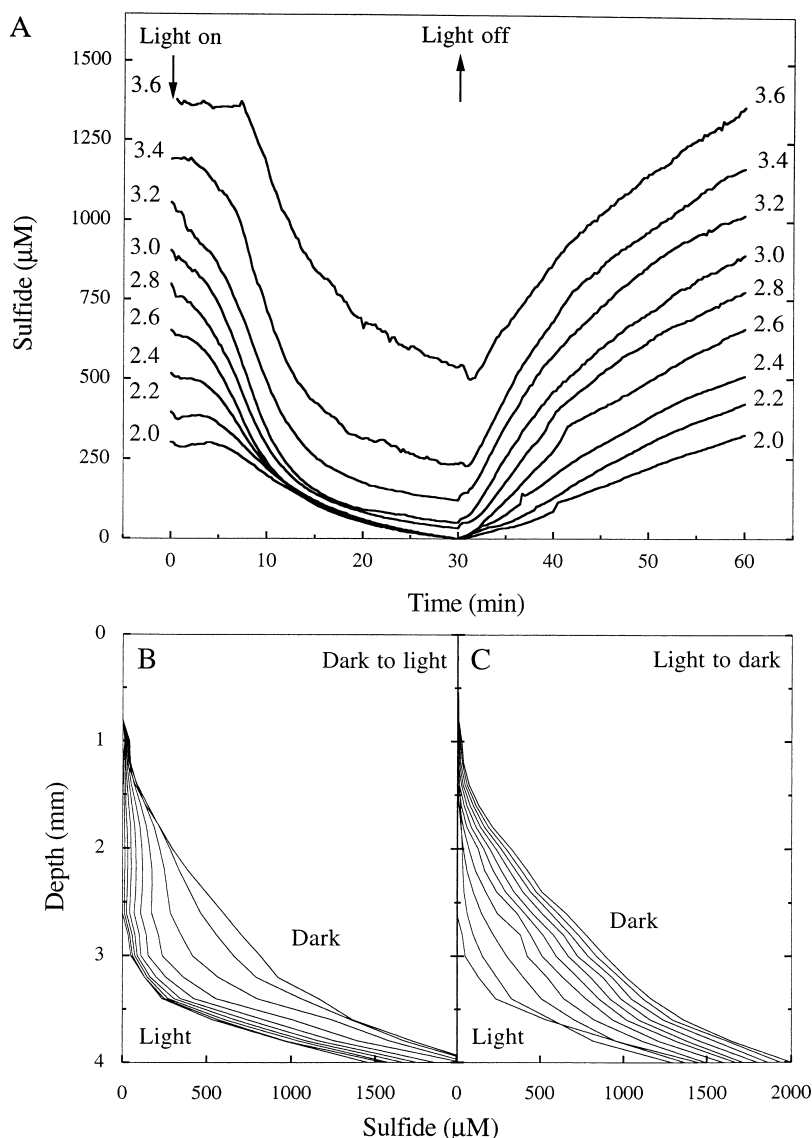


Fig. 4. A. Sulphide variations for selected depths (indicated by number on graph) during light–dark shift of 30 min in a biofilm of *Prosthecochloris aestuarii*. Selected reconstruction of transient sulphide profiles obtained during the light–dark cycles. B. From dark to light. C. From light to dark. The delay between two profiles is 1 min.

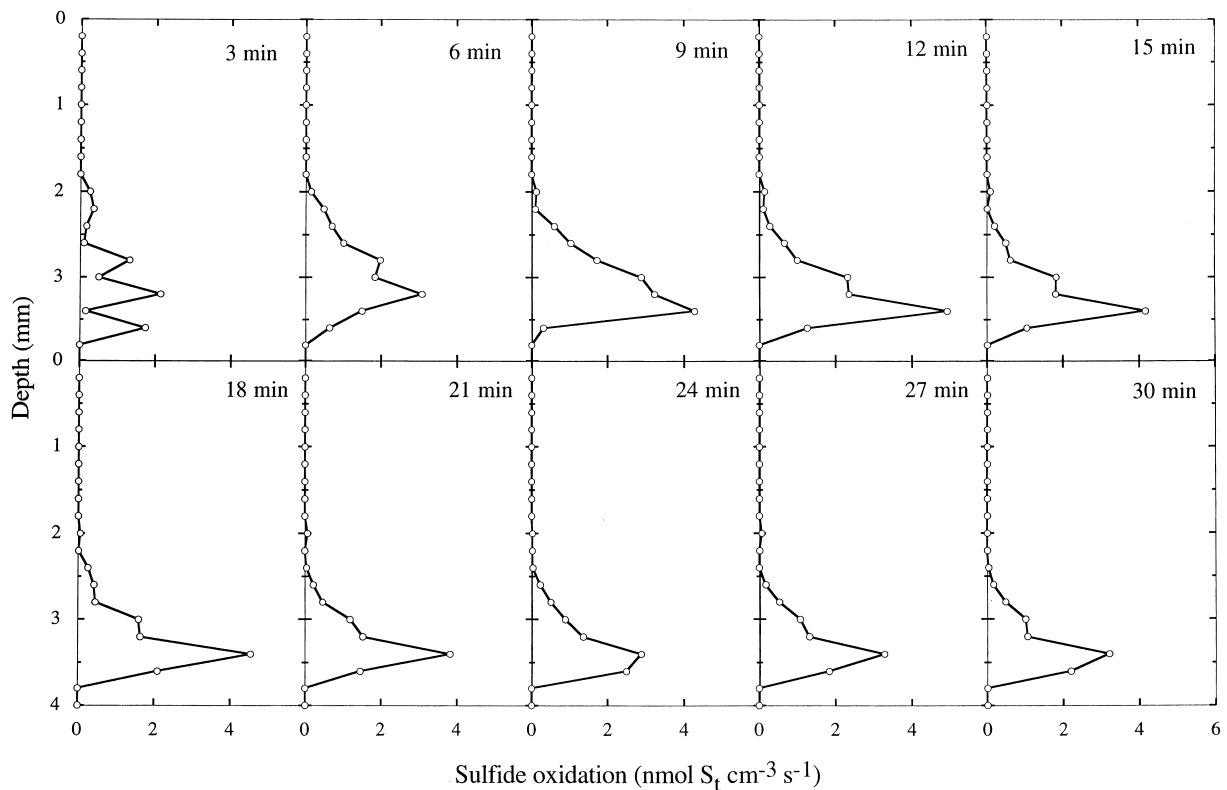


Fig. 5. Depth distribution of the anoxygenic photosynthesis within a biofilm of *Prosthecochloris aestuarii* for different times after exposure to light.

the transient profiles (data not shown). These findings support the assumption that *P. aestuarii* was growing photolithotrophically.

The rates of anoxygenic photosynthesis as a function of depth and time were calculated from the sulphide concentration changes along vertical profiles after light exposure using eqn 4. The anoxygenic photosynthesis profile for different times after light exposure is shown in Fig. 5. Anoxygenic photosynthesis showed an increase with depth, with a maximum value of $5.2 \text{ nmol } S_t \text{ cm}^{-3} \text{ s}^{-1}$ at 3.4 mm, after 12 min of light exposure. Below this depth, no significant anoxygenic photosynthesis was observed. During the first 12 min, anoxygenic photosynthesis increased with time at all depths in the biofilm. Subsequently, a decrease was observed, being more pronounced in the uppermost layers. In the bottom layers, sulphide consumption persisted even after 30 min of light exposure. The areal rate of anoxygenic photosynthesis estimated by summing the activities after correction for porosity was $0.083 \text{ nmol cm}^{-2} \text{ s}^{-1}$ just before darkening. Figure 6 shows the sulphide oxidation rate versus time and the actual sulphide concentration for different layers in the *P. aestuarii* biofilm. The plots of anoxygenic photosynthesis versus time showed similar trends for all layers; a maximum was reached after 8–10 min of light exposure, followed immediately by a decrease.

Discussion

Examining the dynamics of anoxygenic photosynthesis was only possible by an appropriate choice of bacterium, sulphide electrode and method, as will be explained in the following paragraph.

Although green sulphur bacteria are not common in benthic systems, *P. aestuarii* is an ideal bacterium for studying the dynamics of anoxygenic photosynthesis because of its metabolic constraints. By cultivating *P. aestuarii* in the BGC, the sulphide decrease upon light exposure can be attributed to anoxygenic photosynthetic activity, without the need to consider competing reactions for sulphide removal. Furthermore, thanks to the use of a phosphate buffer, variations in H_2S signals upon light or dark exposure cannot be attributed to a change in pH, as has been observed previously in similar biofilms in which a sharp increase in pH occurred immediately upon light exposure. Concomitantly, the H_2S concentration decreased. However, discrimination between the effects of pH and bacterial activity was difficult to resolve (Pringault *et al.*, 1998).

In this study, the newly developed H_2S microsensors were used to measure the sulphide concentration. This sensor offers several advantages over the conventional potentiometric pS^{2-} microsensors for determining anoxygenic photosynthesis. As the amperometric microsensors measure

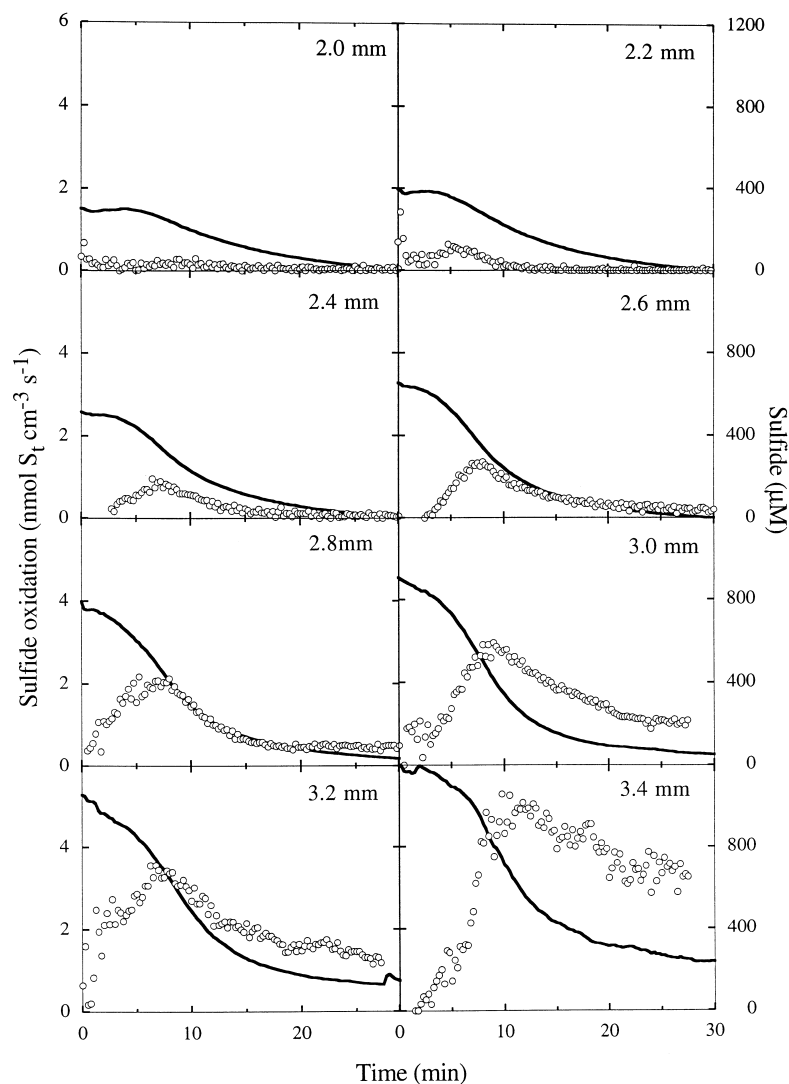


Fig. 6. Changes in anoxygenic photosynthesis (\circ) as a function of time for selected depths (indicated by number on graphs) within the biofilm of *Prosthecochloris aestuarii*. The sulphide concentrations (solid line) are also depicted to visualize the availability of the substrate within the layer.

H_2S directly and as the pK_1 is well defined (Millero *et al.*, 1988), the sum of $\text{H}_2\text{S} + \text{HS}^-$ can be determined accurately, in contrast to calculations based on S^{2-} measurements, which require the ill-defined pK_2 value (Millero, 1986). In addition, the amperometric microsensor has a fast response time, which allows an accurate tracing of the sulphide concentration. The potentiometric sensor typically has a long response time, increasing at lower sulphide concentrations (Kühl and Jørgensen, 1992a), which renders it unsuitable for rate measurements. Caumette *et al.* (1994) have applied the light–dark shift method, originally developed to measure gross rates of oxygenic photosynthesis, to calculate anoxygenic photosynthesis in a dense layer of purple sulphur bacteria using a potentiometric S^{2-} sensor. The vertical resolution of this method is governed by the Einstein–Smoluchowski equation (Revsbech and Jørgensen, 1983):

$$s = (2D_s t)^{0.5} \quad (1)$$

where s represents the vertical migration of the molecules during t seconds. With a sulphide diffusion coefficient of $7.56 \times 10^{-5} \text{ cm}^2 \text{ s}^{-1}$ calculated for this study and a light exposure of 5 min, which is the average response time for a potentiometric sensor, s would be 0.673 mm. Therefore, the vertical resolution between two measurements would be greater than 0.7 mm, which significantly limits the application of the potentiometric sensor in studies on anoxygenic photosynthesis.

Diffusion coefficient of sulphide

The dynamics in transient H_2S profiles depend not only on activity, but on diffusion as well. Therefore, it was essential to quantify D_s in the sediment used for the cultivation of *P. aestuarii*. Using the method described by Revsbech (1989a), an estimation of the diffusivity of H_2S can be obtained. As H_2S is a weak diprotic acid, the pH gradient,

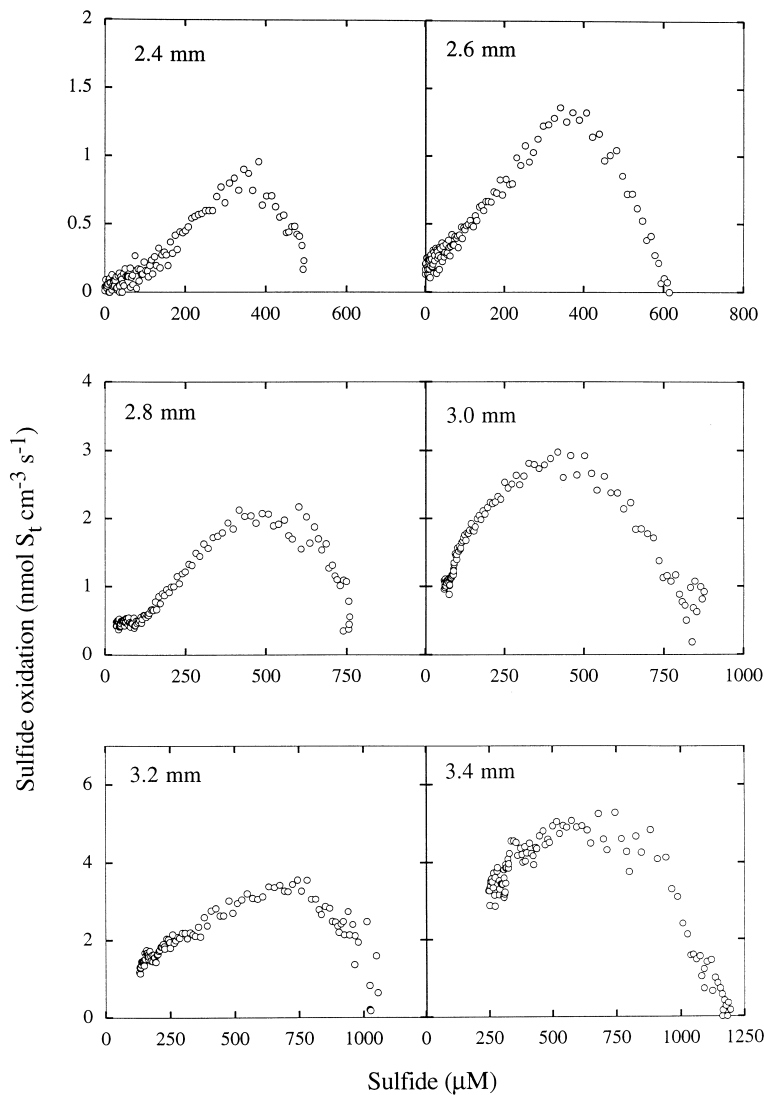


Fig. 7. Relationship between anoxygenic photosynthesis and sulphide concentration for selected depths (indicated by number on graphs) within the biofilm of *Prosthecochloris aestuarii*.

the dissociation kinetics and the differential mobility of the chemical species will govern the distribution of H_2S , HS^- and S^{2-} . The relation between diffusion process and chemical reaction kinetics is given by the Damkhöler number, defined as the ratio of the time scale of the chemical kinetic reaction and the time scale of the diffusion process (Bennani *et al.*, 1981). In experimental situations, large Damkhöler numbers characterize a process controlled by the kinetic of the chemical reaction; on the contrary, for small Damkhöler numbers, the diffusion process becomes the leading parameter. H_2S has a small Damkhöler number, indicating that the estimation of the sum of $\text{H}_2\text{S} + \text{HS}^-$ is not limited by the dissociation of H_2S in sea water. For the carbonate system, the hydration of CO_2 in water is a very slow process, resulting in a high Damkhöler number, thus excluding a precise determination of the sum of the carbonate system species from the CO_2 concentration (De Beer *et al.*, 1997). For the sulphide

system, owing to a small Damkhöler number for H_2S , linear gradients can be expected in the diffusion coefficient experiment and, therefore, a precise estimation of D_s for H_2S can be inferred from this concentration gradient (Fig. 1). In order to check the accuracy of the estimation of D_s for H_2S , D_s was also estimated for O_2 in the same sand (data not shown). The ratio $D_s(\text{O}_2)/D_s(\text{H}_2\text{S})$ was equal to 1.325, a value similar to the $D_o(\text{O}_2)/D_o(\text{H}_2\text{S})$ ratio calculated from the table in Broecker and Peng (1974). Nelson *et al.* (1986) have measured a D_s value for H_2S in agar (0.4% w/v) of $1.39 \times 10^{-5} \text{ cm}^2 \text{ s}^{-1}$ at room temperature (22–25°C), a value 16% lower than D_o ($1.65 \times 10^{-5} \text{ cm}^2 \text{ s}^{-1}$). According to Revsbech (1989a), the diffusion in a low concentration of agar (0.2–2%, w/v) should be the same as the diffusion in water. The data obtained from Nelson *et al.* (1986) demonstrate the difficulty of estimating the sulphide diffusion coefficient accurately in benthic environments.

The determination of anoxygenic photosynthesis

Owing to the fast equilibration of H_2S in sea water, the rate of anoxygenic photosynthesis can be determined by summing the fluxes of H_2S and HS^- , where the latter is calculated from the measured H_2S and pH. The rate of anoxygenic photosynthesis in the *P. aestuarii* biofilm was calculated for the steady-state condition before cycling and for the dynamic conditions during cycling. From the steady-state H_2S and pH profile in light, an areal rate of $0.079 \text{ nmol cm}^{-2} \text{ s}^{-1}$ was calculated. The H_2S profile indicated that only the lower part of the biofilm was involved in the removal of sulphide (Fig. 2A). During steady state in darkness, however, the upper part of the biofilm was exposed to sulphide as well (Fig. 2B), which allowed the bacteria from this layer to oxidize sulphide temporarily upon illumination. The contribution of the upper biofilm to sulphide removal was shown by the analysis of the transient profiles from the cycling experiment. Upon illumination, a thick layer of the biofilm was involved in anoxygenic photosynthesis (Fig. 5), which consumed the standing stock of sulphide accumulated during darkness. However, the thickness of the active layer reduced with time (Fig. 5), as areal anoxygenic photosynthesis and the upward flux of sulphide approached steady state. The areal rate calculated from the cycling procedure just before darkening was $0.083 \text{ nmol cm}^{-2} \text{ s}^{-1}$. This rate is similar to the value calculated from the steady state before cycling, indicating that the system was in steady state after 30 min of light exposure.

Anoxygenic photosynthesis distribution within the biofilm

The vertical radiance attenuation profile for 750 nm provides a proxy for the *P. aestuarii* distribution within the sediment. This profile showed that the bacteria were located below the maximum oxygen penetration. The biofilm could be divided into two sublayers with respect to substrate availability and activity. The upper layer, exposed to sulphide during darkness and the early stage of illumination, only oxidized sulphide transiently upon illumination, whereas the deeper population was permanently exposed to sulphide and involved in anoxygenic photosynthesis during illumination. The difference in sulphide availability for anoxygenic photosynthesis will affect the growth yield in the different sublayers. If sulphide is available, it is oxidized to elemental sulphur, which is stored extracellularly in green sulphur bacteria. Once sulphide is depleted, these bacteria may oxidize their extracellular elemental sulphur to sulphate. Energetically, the oxidation of elemental sulphur to sulphate is more efficient than the initial step of anoxygenic photosynthesis, i.e. oxidation of sulphide to elemental sulphur (Brune, 1989).

Therefore, the bacteria that are located in the upper layer, where sulphide is completely depleted during light exposure, may have a higher growth yield on sulphide than those located at the bottom of the biofilm where sulphide is always available.

The anoxygenic photosynthesis rate for a defined layer of the *P. aestuarii* biofilm can be plotted versus the actual sulphide concentration within the same layer. In this way, the anoxygenic photosynthesis rate can be compared directly with the sulphide concentration (Fig. 7). Similar trends were observed for the different layers of the biofilm; a linear increase in anoxygenic photosynthesis with increasing sulphide concentrations up to a maximum rate and a subsequent decline in activity, suggesting substrate inhibition at high sulphide concentrations. The different layers of the biofilm exhibited an apparent inhibition effect at a sulphide concentration range of 550–1200 μM (Fig. 7). Green sulphur bacteria are known to be inhibited by sulphide concentrations of 5–10 mM (Van Gemerden, 1984; Brune, 1989), which are much higher than the range of apparent inhibition concentrations observed in the experimental *P. aestuarii* biofilm. This apparent inhibition effect calls for a different hypothesis and interpretation. Upon illumination, the bacteria in the upper layers of the biofilm were confronted with strong light radiation (i.e. $230 \mu\text{mol photons m}^{-2} \text{ s}^{-1}$), which was much higher than the saturation value ($4 \mu\text{mol photons m}^{-2} \text{ s}^{-1}$) calculated for this biofilm cultured under similar conditions (Pringault *et al.*, 1998). It is speculated that these bacteria, being non-motile and therefore unable to escape unfavourable light conditions periodically, had to rearrange their light-harvesting pigments to protect themselves against this high light radiation (J. Kuever, personal communication). Therefore, the lag time observed upon illumination before maximum anoxygenic photosynthesis (Fig. 6) could be interpreted as light inhibition causing a time-dependent reorganization of the photopigments. For the different layers, a lag time of 8–10 min was observed before the maximum anoxygenic photosynthesis. This effect was more pronounced in the upper layers, in which a delay of 4–6 min was observed before a net anoxygenic photosynthesis could be measured. As a consequence, the apparent inhibitory effect of sulphide (Fig. 7) could be explained in the upper layers by the time observed consecutively to the light exposure. The bacteria were exposed to a high sulphide concentration at the beginning of the light period, which decreased slowly in the first minutes upon illumination as a result of low phototrophic oxidation. This low activity could be caused by a time-dependent reorganization of pigments imposed by the strong light radiation.

The lower layers showed an immediate response after light exposure, with an increase in activity with time. This immediate response demonstrates that the bacteria are

not affected by strong light radiation and, therefore, they can oxidize sulphide immediately when exposed to light. The lag before maximum rates of sulphide oxidation upon switching on light could be explained tentatively as a result of competition between cyclic and non-cyclic electron transport in green sulphur bacteria. Because green sulphur bacteria have no fermentative or respiratory energy-yielding metabolism in darkness, it is anticipated that their energy charge and their proton motive force (pmf) across the cytoplasmic membrane decrease to very low levels. Presumably, upon switching on the light, a low pmf favours cyclic electron transport (no oxidation of sulphide) over reduction until a sufficiently high pmf has been re-established (apparently 5–10 min is required).

Concluding remarks

The steady-state and the numerical approaches yielded similar areal rates for anoxygenic photosynthesis, confirming that the numerical procedure was well adapted for the study of the dynamics of anoxygenic photosynthesis in an experimental biofilm. The lag time observed before the maximum rate was recorded renders the traditional light–dark shift technique useless for the determination of anoxygenic photosynthesis. This method would require too long light exposures and, therefore, the spatial resolution would be very limited. Although the cycling technique may seem appropriate for determining the rate of anoxygenic photosynthesis in artificial gradient systems, it may prove to be unsuitable for natural systems with more complex sulphur chemistry. The technique may still give an accurate estimate of sulphide removal kinetics, but it will require concurrent measurements of other chemical species to constrain the different processes involved. Currently, some applications of this method are performed to estimate the dynamics of sulphide in microbial mats.

Experimental procedures

Bacterial strains

Prosthecochloris aestuarii strain CE 2401 was cultured in the BGC (for more details, see Pringault *et al.*, 1996). This strain from the Arcachon culture collection is a non-motile bacterium able to grow photolithotrophically with sulphide or elemental sulphur as electron donor. Growth does not occur with thiosulphate as an electron donor and is inhibited by sulphite. The strain is very sensitive to molecular oxygen, which inhibits its growth (Guyoneaud *et al.*, 1996). During the assembly of the BGC, the top centimetre of the sterile sand column was evenly inoculated with a small volume (10 ml) of a batch culture of *P. aestuarii* in logarithmic growth phase.

Culture conditions

The culture device used in this study is a modified version of the BGC described previously (Pringault *et al.*, 1996). It consists

of a 45-mm-long artificial sediment core (internal diameter 50 mm) sandwiched between an upper oxic and a lower anoxic chamber of 2000 ml and 3500 ml respectively. The composition of the two media and the light conditions were the same as those described previously (Pringault *et al.*, 1996; 1998). Air saturation in the upper compartment (230 μM oxygen) was achieved thanks to a sterile air lift (Pringault *et al.*, 1996). Transport of solutes through the sediment core was caused exclusively by molecular diffusion (Pringault *et al.*, 1996). The sand (Merck) had a grain size of 125–250 μm .

Fibre-optic measurements

A field radiance microprobe (Kühl and Jørgensen, 1992b; 1994) was used to identify the vertical position of the phototrophic biofilm. Depth profiles of backscattered radiance were measured at 150° zenith angle relative to the incident light by penetrating the sediment surface from the surface in vertical steps of 100 μm . Backscattered radiance measurements were normalized to the values measured at the sediment surface. The position of the phototrophic biofilm was deduced from attenuation profiles of backscattered radiance at 750 nm, which corresponds to the *in vivo* absorption maxima of bacteriochlorophyll *c* (Bchl *c*), a specific photopigment of *P. aestuarii*. More detailed explanations about the light calculations are given in Pringault *et al.* (1998).

Microelectrodes

O₂, pH and H₂S profiles were measured with microelectrodes. The calibration procedures for the different types of electrodes have been described previously (Pringault *et al.*, 1998). Details about the characteristics of the microelectrodes are given below.

Oxygen microelectrode. The concentration profiles of oxygen were measured by a Clark-type oxygen microelectrode with a guard cathode (Revsbech, 1989b). The electrodes had a tip diameter of 10–20 μm and were connected to a high-impedance picoammeter and a recorder. The stirring sensitivity was < 1%, and the 90% response time was < 1 s.

pH electrode. pH profiles were measured using a pH glass microelectrode (Revsbech and Jørgensen, 1986) connected to a high-impedance electrometer with a calomel electrode (Radiometer) as a reference. The pH microelectrodes showed a log-linear response for H⁺ with a slope of 53–58 mV pH⁻¹ unit and a 90% response time of < 10–20 s.

Hydrogen sulphide microsensor. Concentration profiles of dissolved hydrogen sulphide were measured by a new amperometric H₂S microelectrode (Jeroschewski *et al.*, 1996; Kühl *et al.*, 1998). The electrodes had a tip diameter of 10–20 μm , a 90% response time < 1–2 s and a stirring sensitivity of < 1–2%. The electrode output current was measured with a high-impedance picoammeter using a polarization voltage of + 85 mV.

Simultaneous measurements were made with a H₂S, a pH and an O₂ microsensor mounted on a single motor-driven micromanipulator (Oriel). The tips of the pH and sulphide

electrodes were positioned < 1 cm apart in the same horizontal plane. A dissection microscope was used to position the tips of the three microsensors at the sediment surface. The positioning of the microsensors, light–dark transitions, data acquisition and statistical analysis of the sensor signals was all performed automatically by custom-made hardware and software routines (Labview, National Instruments).

Diffusion measurements

The whole-sediment diffusion coefficient, D_s , for H_2S was estimated for the sand used for the culture in the BGC using the same procedure as described previously (Revsbech, 1989a; Glud *et al.*, 1995). The diffusion chamber described by Revsbech (1989a) was modified to allow the circulation of an anoxic phosphate buffer solution (25 mM, pH 7.2) above the sediment surface, in order to avoid oxygen contamination and to ensure a stable pH (Fig. 1A). Sediment anoxia was verified by oxygen microsensor measurements throughout the sulphide diffusion experiments. The whole-sediment coefficient, D_s , was calculated from the ratio of the concentration gradients in the agar phase and in the sediment phase (Revsbech, 1989a; Glud *et al.*, 1995), assuming steady-state conditions.

Light–dark cycles

The theory and the procedure of the light–dark cycles are given in detail for the oxygen dynamics by E. Epping *et al.* (unpublished). The application for the sulphide dynamics is summarized below.

Theory. The sulphide distribution in the sand core is governed by processes that affect the concentration of sulphide and the diffusive transport of sulphide. Assuming a constant depth distribution of porosity, ϕ , and sediment diffusion coefficient, D_s , the sulphide concentration as a function of time t and depth z , $C(z,t)$, can be expressed by Fick's second law of diffusion:

$$\frac{\partial C(z,t)}{\partial t} = D_s \frac{\partial^2 C(z,t)}{\partial z^2} + P(z,t) - K(z,t) \quad (2)$$

$P(z,t)$ and $K(z,t)$ represent the rate of sulphide production and the rate of sulphide oxidation by microbial and chemical processes at depth z and time t respectively. As *P. aestuarii* is a strictly photolithotrophic bacterium, the sulphide production rate equals zero, which simplifies eqn 2 to:

$$\frac{\partial C(z,t)}{\partial t} = D_s \frac{\partial^2 C}{\partial z^2} - K(z,t) \quad (3)$$

During illumination, the rate of sulphide oxidation resulting from anoxygenic photosynthesis below the oxic layers is represented by:

$$K(z,t) = D_s \frac{\partial^2 C}{\partial z^2} - \frac{\partial C(z,t)}{\partial t} \quad (4)$$

Thus, the rate of anoxygenic photosynthesis as a function of depth and time can be calculated from the second derivative of the sulphide concentration as a function of depth and the rate of change in sulphide concentration resulting from the light exposure of the biofilm.

Procedure. Microsensor measurements were performed after an incubation time of 6 weeks. The system was opened to allow the insertion of optical and chemical microsensors. The system was checked by microscopy for contamination. The number of contaminants was always less than 5% of the total cells per field of observation. In order to reduce the pH variations observed previously during the light and dark periods (Pringault *et al.*, 1998), the oxic medium was replaced by a phosphate buffer (100 mM, pH 7.3) amended with 30 g l^{-1} NaCl.

The oxygen, sulphide and pH microsensors were positioned at a depth of 4.0 mm (below the biofilm). Immediately after positioning the electrodes, the light was turned on for a period of 30 min. The signals of both sensors were recorded every 15 s for 1 s at a sampling frequency of 510 Hz. At the end of this 30 min period, the light was turned off for a dark period of 30 min. After 30 min of exposure to darkness, the two electrodes moved up $200 \mu\text{m}$, and a new light–dark cycle was recorded. This procedure was repeated up to the sediment surface. The signals were converted to sulphide concentration as a function of time and depth, taking into account the pH variations, using the calibration procedure described previously (Pringault *et al.*, 1998). These data were used to calculate the rate of anoxygenic photosynthesis as a function of time and depth using eqn 4.

Acknowledgements

Gaby Eickert, Anja Eggers and Vera Hübner are thanked for the construction of microsensors. Special thanks to R. de Wit for the revision of the initial manuscript. J. Kuever is also thanked for his comments. Part of this study was supported by the Red Sea Research Programme, Project E 'Microbial activities in hypersaline interfaces controlling nutrient fluxes', financed by the German Ministry for Research and Development (BMBF).

References

- Bennani, A., Alcaraz, E., and Mathieu, J. (1981) An experimental set-up for interaction turbulence–chemical reaction research. *Int J Heat Mass Transfer* **24**: 1549–1553.
- Broecker, W.S., and Peng, T.H. (1974) Gas exchange rates between air and sea. *Tellus* **26**: 21–35.
- Brune, D.C. (1989) Sulfur oxidation by phototrophic bacteria. *Biochim Biophys Acta* **975**: 189–221.
- Caumette, P., Matheron, R., Raymond, N., and Relexans, J.C. (1994) Microbial mats in the hypersaline ponds of Mediterranean salterns (Salins-de-Giraud, France). *FEMS Microbiol Ecol* **13**: 273–286.
- De Beer, D., Glud, A., Epping, E., and Kühl, M. (1997) A fast-responding CO_2 microelectrode for profiling sediments, microbial mats, and biofilms. *Limnol Oceanogr* **42**: 1590–1600.
- Fenchel, T. (1998) Artificial cyanobacterial mats: cycling of C, O and S. *Aquat Microb Ecol* **14**: 253–259.
- Glud, R.N., Jensen, K., and Revsbech, N.P. (1995) Diffusivity in superficial sediments and benthic mats determined by use of a combined N_2O – O_2 microsensor. *Geochim Cosmochim Acta* **59**: 231–237.

- Guyoneaud, R., Matheron, R., Baulaigue, R., Podeur, K., Hirschler, A., and Caumette, P. (1996) Anoxygenic phototrophic bacteria in eutrophic coastal lagoons of the French Mediterranean and Atlantic coasts (Prévost Lagoon, Arca-chon Bay, Certes fishponds). *Hydrobiology* **329**: 33–43.
- Jeroschewski, P., Steuckart, C., and Kühl, M. (1996) An amperometric microsensor for the determination of H₂S in aquatic environments. *Anal Chem* **24**: 4351–4357.
- Jørgensen, B.B., and Des Marais, D.J. (1986) Competition for sulfide among colorless and purple sulfur bacteria in cyanobacterial mats. *FEMS Microbiol Ecol* **38**: 179–186.
- King, G.M. (1990) Effects of added manganese and ferric oxides on sulfate reduction and sulfide oxidation in intertidal sediments. *FEMS Microbiol Ecol* **73**: 131–138.
- Kühl, M., and Jørgensen, B.B. (1992a) Microsensor measurements of sulfate reduction and sulfide oxidation in a compact microbial communities of aerobic biofilms. *Appl Environ Microbiol* **58**: 1164–1174.
- Kühl, M., and Jørgensen, B.B. (1992b) Spectral light measurements in microbenthic phototrophic communities with a fiber-optic microprobe coupled to a sensitive diode array detector. *Limnol Oceanogr* **37**: 1813–1823.
- Kühl, M., and Jørgensen, B.B. (1994) The light field of microbenthic communities: radiance distribution and micro-scale optics of sandy coastal sediments. *Limnol Oceanogr* **39**: 1368–1398.
- Kühl, M., Steuckart, C., Eickert, G., and Jeroschewski, P. (1998) A H₂S microsensor for profiling biofilms and sediments: application in an acidic lake sediment. *Aquat Microb Ecol* **15**: 201–209.
- Millero, F.J. (1986) The thermodynamics and kinetics of the hydrogen sulfide system in natural waters. *Mar Chem* **18**: 121–147.
- Millero, F.J. (1991) The oxidation of H₂S in Framvaren Fjord. *Limnol Oceanogr* **36**: 1007–1014.
- Millero, F.J., Plese, T., and Fernandez, M. (1988) The dissociation of hydrogen sulfide in seawater. *Limnol Oceanogr* **33**: 269–274.
- Nelson, D.C., Jørgensen, B.B., and Revsbech, N.P. (1986) Growth pattern and yield of a chemoautotrophic *Beggiatoa* sp. in oxygen–sulfide microgradients. *Appl Environ Microbiol* **52**: 225–233.
- Nicholson, J.A., Stolz, J.F., and Pierson, B.K. (1987) Structure of microbial mat at Great Sippewissett Marsh, Cape Cod, Massachusetts. *FEMS Microbiol Ecol* **45**: 343–364.
- Pierson, B.K., Oesterle, A., and Murphy, G.L. (1987) Pigments, light penetration and photosynthetic activity in the multilayered microbial mats of great Sippewissett salt marsh. *FEMS Microbiol Ecol* **45**: 365–376.
- Pierson, B.K., Sands, V.M., and Frederick, J.L. (1990) Spectral irradiance and distribution of pigments in a highly layered marine microbial mat. *Appl Environ Microbiol* **56**: 2327–2340.
- Pringault, O., De Wit, R., and Caumette, P. (1996) A Benthic Gradient Chamber for culturing phototrophic sulfur bacteria on reconstituted sediments. *FEMS Microbiol Ecol* **20**: 237–250.
- Pringault, O., Kühl, M., De Wit, R., and Caumette, P. (1998) Growth of green sulfur bacteria in experimental benthic oxygen, sulphide, pH and light gradients. *Microbiology* **144**: 1051–1061.
- Revsbech, N.P. (1989a) Diffusion characteristics of microbial communities determined by use of oxygen microsensors. *J Microbiol Methods* **9**: 111–122.
- Revsbech, N.P. (1989b) An oxygen microsensor with a guard cathode. *Limnol Oceanogr* **34**: 472–476.
- Revsbech, N.P., and Jørgensen, B.B. (1983) Photosynthesis of benthic microflora measured with high spatial resolution by the oxygen microprofile method: capabilities and limitations of the method. *Limnol Oceanogr* **28**: 749–756.
- Revsbech, N.P., and Jørgensen, B.B. (1986) Micro-electrodes: their use in microbial ecology. *Adv Microb Ecol* **9**: 293–352.
- Skyring, G.W. (1987) Sulfate reduction in coastal ecosystems. *Geomicrobiol J* **5**: 295–374.
- Stolz, J.F. (1990) Distribution of phototrophic microbes in the flat laminated microbial mat at Laguna Figueroa, Baja California, Mexico. *Biosystems* **23**: 345–357.
- Stumm, W., and Morgan, J.J. (1981) *Aquatic Chemistry. An Introduction Emphasizing Chemical Equilibria in Natural Waters*. New York: Wiley.
- Thamdrup, B., Finster, K., Hansen, J.W., and Bak, F. (1993) Bacterial disproportionation of elemental sulfur coupled to chemical reduction of iron manganese. *Appl Environ Microbiol* **59**: 101–108.
- Van Gernerden, H. (1984) The sulfide affinity of phototrophic bacteria in the relation to the location of elemental sulfur. *Arch Microbiol* **139**: 289–294.
- Van Gernerden, H. (1993) Microbial mats: a joint venture. *Mar Geol* **113**: 3–25.
- Van Gernerden, H., and Mas, J. (1995) Ecology of phototrophic sulfur bacteria. In *Anoxygenic Photosynthetic Bacteria*. Blankenship, R.E., Madigan, M.T., and Bauer, C.E. (eds). Dordrecht: Kluwer Academic Publishers, pp. 49–85.
- Visscher, P.T., Van Den Ende, F.P., Schaub, B.E.M., and Van Gernerden, H. (1992) Competition between anoxygenic phototrophic bacteria and colorless sulfur bacteria in a marine microbial mat. *FEMS Microbiol Ecol* **101**: 51–58.